Role of Mesenchymal Stem Cells Transfected With Vascular Endothelial Growth Factor in Maintaining Renal Structure and Function in Rats with Unilateral Ureteral Obstruction

Emin Ozbek,[1] Gokhan Adas,[2] Alper Otunctemur,[1] Gokhan Duruksu,[3] Bora Koc,[2] Emre Can Polat,[4] Ahu Kemik Sarvan,[5] Alparslan Okcu,[3] Gulcin Kamali,[6] Cansu Subasi,[3] Erdal Karaoz[7]

Abstract

Objectives: Mesenchymal stem cells hold promise for renal disease treatment. Vascular endothelial growth factor may heal tubule-interstitial fibrosis in unilateral ureteral obstruction by inhibiting epithelial-mesenchymal transition. We investigated the protective effect of vascular endothelial growth factor in transfected mesenchymal stem cells in unilateral ureteral obstruction-induced renal injury in rats.

Materials and Methods: Male Wistar Albino rats (32 rats; weight, 250-300 g) were divided into 4 equal groups: group 1, control; group 2, unilateral ureteral obstruction; group 3, unilateral ureteral obstruction and mesenchymal stem cells; and group 4, unilateral ureteral obstruction and vascular endothelial growth factor-transfected mesenchymal stem cells. Vascular endothelial growth factor-transfected mesenchymal stem cells were administered intravenously before onset of unilateral ureteral obstruction. On day 14, the rats were killed and kidneys were retrieved.

Tubular necrosis, mono-nuclear cell infiltration, and interstitial fibrosis were evaluated in paraffin blocks. We evaluated green fluorescent protein-positive and vascular endothelial growth factor-positive cells; anti-inflammatory (Prostaglandin E2 Receptor) and interleukin 1 receptor antagonist), proinflammatory/anti-inflammatory (interleukin 6), and proinflammatory (MPO) cytokine expression levels; and levels of nitric oxide; transforming growth factor β1, E-cadherin, and hydroxyproline.

Results: Green fluorescent protein-positive cells were negative in the renal parenchyma in groups 1 and 2 and positive in groups 3 and 4. Vascular endothelial growth factor levels were significantly higher in group 4. Transforming growth factor β1, nitric oxide, and E-cadherin levels were significantly higher in the unilateral ureteral obstruction than control group; however, in the study groups, these values were not significantly different from the unilateral ureteral obstruction group. In stem cell-transplanted tissue samples, EP3, interleukin 1 receptor antagonist, and interleukin 6 levels were elevated, but MPO expression levels were low. Although there were significant differences for tubular necrosis and fibrosis in group 2, there were significant reductions in tubular injury and fibrosis in groups 3 and 4.

Conclusions: Systemic stem cells transplanted into the kidney protected against unilateral ureteral obstruction-induced renal epithelial-mesenchymal transition and renal fibrosis.

Key words: Epithelial-mesenchymal transition, Renal injury, Obstructive nephropathy, Ureter obstruction

DOI: 10.6002/ect.2014.0080

Introduction

Ureteral obstruction occurs at any stage of life from fetal development until adult life in any segment of the ureter between the ureteral orifices and renal pelvis. Both the degree (partial or complete) and duration of obstruction (acute or chronic) are responsible for the affect. Obstructive nephropathy, which is characterized by the development of tubule-interstitial fibrosis, is a common cause of renal failure or end-stage renal disease in adults and children. Interstitial fibrosis is a complex pathophysiologic process that involves inflammatory cell infiltration, fibroblast proliferation, and an imbalance between extracellular matrix synthesis and degradation.[1,2]

In an animal model of unilateral ureteral obstruction (UUO), the pathophysiology of ureteral obstruction-induced renal injury has been well studied. In the UUO model, chronic ureteral obstruction-induced renal fibrosis injures the renal tubules. In the early stage, this injury is mediated by macrophages. In the late stages of obstruction, injury is mediated by both transforming growth factor β1 (TGF-β1) and an imbalance between extracellular matrix synthesis and degradation due to increased fibroblast proliferation.[1,2]Activated fibroblasts are the principal effector cells responsible for extracellular matrix deposition and development of tubule-interstitial fibrosis. Furthermore, recent evidence suggests that growth factors, such as TGF-β1, can induce renal tubular epithelial cells to undergo phenotypic transformation into matrix-producing myofibroblasts under pathologic conditions, known as epithelial-mesenchymal transition (EMT).[3,4] Renal cortical TGF-β1 levels increase significantly in response to obstruction, and TGF-β1 is a major regulator of fibrosis by stimulating EMT, fibroblast proliferation, and extracellular matrix synthesis.[1]

Several agents have been used to prevent UUO-induced renal injury in animal models, but there are few experiments regarding the role of stem cells.[5-8] Mesenchymal stem cells (MSCs) have been used in a rodent model of UUO.[7-11] Major mechanisms with therapeutic implications for stem cells include the inhibition of EMT, immunosuppression, and anti-inflammatory effects.[10-12] In addition, MSC transplant causes decreased fibrosis in the heart, lung, liver, and kidney in experimental animal models.[8,13-16] These results suggest that the beneficial effect is attributable to a reduction in the rejection by MSCs.

In the present study, we aimed to investigate the therapeutic effects of rat MSCs and MSCs transfected with vascular endothelial growth factor (VEGF). We evaluated the effect of both the cell line (MSCs and transfected MSCs) during ureteral obstruction and the possible preventive mechanisms of action of MSCs on renal damage in rats. In addition, we determined the role of stem cells and VEGF-transfected MSCs in facilitating kidney regeneration.

Materials and Methods

Animals
This study was completed in the Department of Experimental Medical Research and Application of Kocaeli University. The Animal and Ethics Review Committee at Kocaeli University evaluated and approved the protocol used in this study according to the institutional and national animal welfare guidelines. The animals were housed under standard conditions before use.

Isolation and culture of bone marrow mesenchymal stem cells
Bone marrow (BM) was removed from twelve, 10- to 12-week-old male Wistar Albino rats as previously described for adherent culture of the BM-MSCs in vitro.[16,17] The femurs and tibias were excised, and the bone cavity was flushed with a standard culture medium using a 21-gauge needle. The marrow plug was suspended in a solution of phosphate-buffered saline (PBS) and separation medium (Histopaque, 1.077 g/mL, Sigma, St. Louis, MO, USA) and was centrifuged at 200 ×g for 10 minutes. The supernatant, which contained thrombocytes and erythrocytes, was discarded, and the cell pellet was resuspended in Dulbecco Modified Eagle Medium (DMEM) (Gibco/Invitrogen, Paisley, United Kingdom). The cells from each rat were seeded in 25-cm^2 plastic tissue culture flasks and incubated under standardized culture conditions (37°C, 5% carbon dioxide, humidified atmosphere) for 3 days. The adherent cells were grown to 70% confluence and were passaged using trypsin (0.25%, Gibco/Invitrogen). These cells were defined as passage zero (P0). Standardized culture medium (DMEM supplemented with 10% fetal bovine serum [Gibco/Invitrogen] and 1% penicillin/streptomycin [Gibco/Invitrogen]) was replaced every 3 days.

Flow cytometry
The BM-MSCs (passage 3 [P3]) were subjected to flow cytometry analysis (FACSCalibur, BD Biosciences, San Jose, CA, USA). Immunophenotyping analysis was performed for the antigens CD29, CD45, CD54, CD90, CD106, major histocompatibility complex (MHC) class I, and MHC class II (BD Biosciences).

In vitro differentiation
To induce adipogenic differentiation, cells (P3; 3000 cells/cm^2) were seeded on coverslips coated with type I collagen (BD Biosciences) in 6-well plates. The adipogenic medium, which was DMEM supplemented with 10% fetal bovine serum, 0.5 isobutyl methylxanthine (IBMX; Sigma), 10 μM dexamethasone (Fluka Chemie AG, Buchs, Switzerland), 10 μg/mL insulin (Invitrogen/-GIBCO), 200 μ indomethacin (Sigma), and 1% penicillin/streptomycin, was used for 4 weeks. The medium was replaced twice weekly. Intracellular lipid droplets, which indicated adipogenic differentiation, were confirmed by Oil Red O stain (0.5% in methanol) (Sigma).

For osteogenic differentiation, cells (P3; 3000 cells/cm^2) were seeded on coverslips coated with type I collagen 6-well plates. The differentiation medium was DMEM supplemented with 10% fetal bovine serum, 0.1 μM dexamethasone (Sigma), 0.05 μM ascorbate-2-phosphate (Wako Chemicals, Richmond, VA, USA), 10 mM β-glycerophosphate (Sigma), and 1% penicillin/streptomycin, and was replaced twice weekly. After 4 weeks, osteogenic differentiation was confirmed by Alizarin Red stain. For Alizarin Red staining, the cells were fixed for 5 minutes in ice-cold 70% ethanol. The cells were stained with Alizarin Red solution (2%; pH 4.2). Stained cells were dehydrated in pure acetone, fixed in an acetone-xylene (1:1) solution, and cleared with xylene.

Green fluorescent protein labeling of stem cells
Stem cells were labeled with green fluorescent protein (GFP) by labeling with pGFP (Clontech, Palo Alto, CA, USA) using a transfection system (Neon, Invitrogen-Life Technologies, Carlsbad, CA, USA) according to the instructions described by the supplier.[16] The cells were washed 3 times with PBS and mixed with pGFP. The transfer parameters were 990 V, 40 ms, and 2 pulses. The stable cell lines were maintained by the continuous culture of transfected cells in the culture media with G418 (Gibco/Life Sciences; 200 μg/mL).

Transfection of vascular endothelial growth factor gene
The VEGF carrying the VEGF-165 gene was provided kindly by Dr. Duran Ustek, Department of Genetics, Institute of Experimental Medicine, Istanbul University. The gene was ligated down-stream of the *cytomegalovirus* promoter of the pGFP vector (Clontech). After excising the GFP gene by restriction digestion. The plasmid of VEGF was cotransfected with pGFP (1:10). The same procedures were used in transfection and selection as described for the GFP-labeling of cells.

Surgical procedure and cell transplant
Male Wistar Albino rats (32 rats; weight, 250-300 g), were divided into 4 equal groups (8 rats each): group 1, control (sham operation); group 2, UUO; group 3, UUO and systemic transplanted MSCs (UUO + MSC); and group 4, UUO and systemic transplanted VEGF and MSCs (UUO + VEGF + MSC). The rats were housed at 21°C and given tap water and rat food. All groups were killed 14 days after the surgical procedure.

All surgical procedures were performed under anesthesia using ketamine hydrochloride (50-100 mg/kg) and under sterile conditions. The UUO was induced as described previously.[18] The left ureter was isolated and ligated using 3-0 silk sutures. In the MSC group, the UUO surgery was performed, and we injected 1 mL allogeneic MSC and VEGF-transfected MSC suspension (1 × 10^6 cells/mL) into the inferior vena cava 10 minutes after ureteral ligation. In the UUO group, the ureters were ligated, and 1 mL saline was injected into the inferior vena cava. Sham-operated controls (group 1) had the abdominal cavity opened and ureter manipulated without any ligation. No antibiotics or analgesics were given before or after the surgical procedure.

At the end of day 14 after surgery, the rats were killed, and the kidneys were removed, snap frozen in liquid nitrogen for biochemical analysis, and fixed for MSC localization and histopathologic examination.

Histopathologic examination
Left nephrectomies were performed on the rats. The tissues were postfixed in 4% formaldehyde

overnight, embedded in paraffin, and sectioned to 4-μm thickness. The sections were stained with hematoxylin and eosin. An experienced pathologist conducted the histologic assessments without knowing the identity of the groups. The kidney sections were analyzed semiquantitatively as previously described.[6] Tubular necrosis, interstitial fibrosis, and mononuclear cell infiltration in the sections were studied and scored from 0 to 3 (0, none; 1, slight; 2, moderate; and 3, dense). Masson trichrome stain was used to distinguish cells from the surrounding connective tissue.

Immunostaining for paraffin sections
Consecutive sections, each 4-μm thick, were taken from paraffin-embedded left kidney samples. To detect GFP-positive and VEGF-positive MSCs, a double immunostaining protocol was followed. Slides were deparaffinized with xylene for 5 minutes twice, and rehydrated in a series of graded alcohol solutions (70%-100%). Endogenous peroxidases were inhibited by incubation with 3% hydrogen peroxide in PBS. Nonspecific staining was blocked with a mixture of serum in 1.5% PBS for 30 minutes at room temperature, and tissue sections were incubated in a mixture of 2 primary antibodies in pairwise fashion with mouse monoclonal anti-GFP antibody (SC-9996 or SC-5385) and VEGF (Thermo Scientific, Fremont, CA, USA) at appropriate dilutions for 1 hour at room temperature. After incubation with appropriate fluorescent-conjugated secondary antibodies, the sections were covered with mounting medium containing 4',6-diamidino-2-phenylindole (DAPI) (Santa Cruz, Heidelberg, Germany).

Measurement of transforming growth factor β1, E-cadherin, nitric oxide, and hydroxyproline levels
The TGF-β1 enzyme-linked immunosorbent assay kit (MB100B, R&D Systems Inc, Minneapolis, MN, USA) was used to measure TGF-β1 in the left renal tissue. Total proteins (50 μg) from each tissue were assayed. This assay detected activated TGF-β1 with a sensitivity of 4.6 pg/mL. The intra-assay coefficient of variation was < 4%, and the interassay coefficient of variation was < 8%.

The concentration of soluble E-cadherin was measured with a commercially available sandwich enzyme-linked immunosorbent assay kit based on monoclonal antibodies (Zymed Laboratories Inc., San Francisco, CA 94080, USA). The intra-assay coefficient

of variation was < 5%, and the interassay coefficient of variation was 7%. The sensitivity was 2.0 ng/mL.

Nitrate concentrations in the samples were assayed by enzymatically reducing nitrate. Each sample (50 μL) was incubated with the same volume of reductase buffer (0.1 M potassium adenine dinucleotide), and 4 units of nitrate curve were obtained by incubating sodium nitrate (10-200 μM) with the buffer. The total amounts of nitrite and nitrate in the samples were then determined using Griess method.[19] The samples were incubated with the same volume of Griess reagent (1% sulphanilamide and 0.1% N-(1-Naphthyl) ethylene-diamine dihydrochloride in 5% phosphoric acid). The absorbance at 550 nm was determined using a multiwell plate reader. The results were reported as concentration of nitrate plus nitrite ($\mu M\ NO_3 + NO_2$) for samples of nitrite supernatants.

Left renal tissue fragments were homogenized in 0.9% saline, frozen, and lyophilized. The assay was performed with 40 mg of lyophilized tissue that was subjected to alkaline hydrolysis in 300 μL plus 75 μL sodium hydroxide (10 M) at 120°C for 20 minutes. An aliquot of 50 μL of the hydrolyzed tissue was added to 450 μL of chloramine T oxidizing reagent (chloramine T [0.056 mmoL/L] and n-propanol [10%] in acetate/citrate buffer, pH 6.5) and allowed to react for 20 minutes. A hydroxyproline standard curve with the highest concentration of 400 μg was prepared likewise. Color was developed by the addition of 500 μL of Ehrlich reagent (p-dimet-hylaminobenzaldehyde, 1 M) diluted in n-propanol/perchloric acid (2:1); the supernatant was transferred to 96-well plates, and the absorbance was measured at 550 nm.

Statistical analyses
The results of all groups were reported as mean ± standard deviation (SD). Statistical analyses of the histopathologic evaluation of the groups were performed using chi-square test, and biochemical data were analyzed with a 1-way analysis of variance. The significance between 2 groups was determined by Dunnett multiple comparison test, and $P \le .05$ was accepted as a statistically significant value.

Results

Culture and characterization of mesenchymal stem cells
Isolated cells from rat bone marrow (rBM) were distributed sparsely on the culture flasks and

displayed mostly fibroblastlike, spindle-shaped morphology during the early days of incubation. Small colonies, termed colony-forming units, appeared within 4 to 7 days (Figure 1), and these primary cells reached monolayer confluence within 12 to 15 days. In the later passages, most of these MSCs exhibited large, flattened, or fibroblastlike morphology (Figure 1).

Flow cytometry analysis data indicated that rBM-MSCs maintained the typical immunologic character of MSCs, expressing CD29, CD54, CD90, and MHC class I but not CD45, CD106, or MHC class II. This phenotypic character was maintained throughout all passages (Figure 1). The isolated cells were incubated in differentiation media for adipocyte and osteocyte formation (Figure 1). Morphologic, histologic, and immunohistochemical analyses showed that the cells differentiated successfully.

Histopathology

In the control group, there were normal tubules and glomeruli in the left kidney cortex; however, there also was slight epithelial vacuolization in the proximal tubules (score 1) and a normal glomerulus in the groups treated with UUO + MSC or UUO + VEGF + MSC. There was severe tubular total necrosis, tubular degeneration, and epithelial vacuolization in the proximal tubules (score 4) in the group 2 and mild epithelial vacuolization in the proximal tubules (score 2) and normal glomerulus in the group 3 and group 4. However, in rats that had UUO, leukocyte infiltration was reduced in the

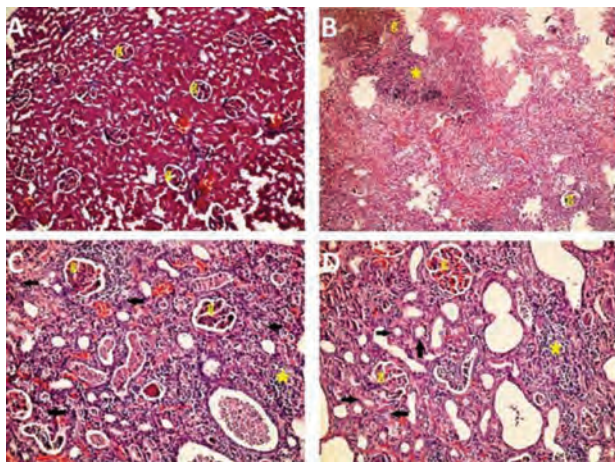**Figure 1.** Rat Bone Marrow Mesenchymal Stem Cell Cultures
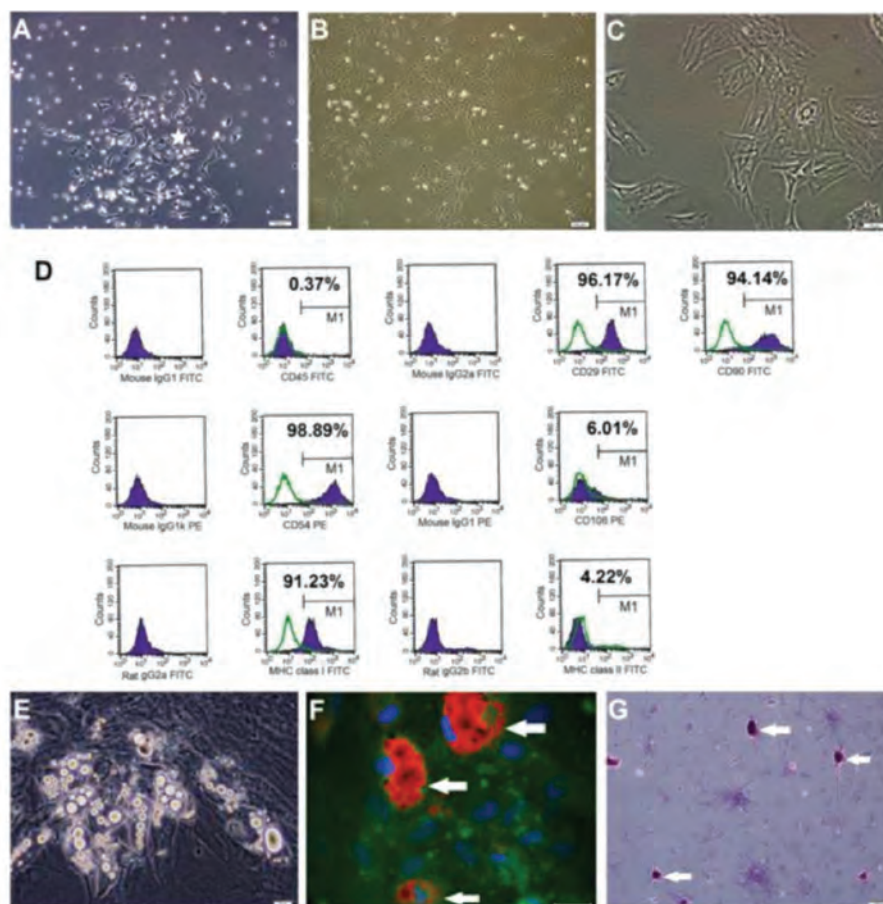
(A) Isolated cells from rat bone marrow (rBM) were distributed sparsely in the culture flasks and displayed mostly fibroblastlike, spindle-shaped morphology during the early days of incubation. Small colonies, termed colony-*forming units (*)*, appeared within 4 to 7 d (A: zero passage, fourth day), and these primary cells reached monolayer confluence within 12 to 15 d. **(B, C)** In the later passages, most of these mesenchymal stem cells (MSCs) exhibited large, flattened, or fibroblastlike morphology **(B)** second passage, eighth day; **(C)** third passage, fourth day). **(D)** Immunophenotypic properties of rBM-MSCs evaluated with flow cytometry. Predefined markers that specified MSCs were used to define the characteristics of cultured cells. The rBM-MSCs expressed all mesenchymal stem cell markers including CD29, CD54, CD90, and major histocompatibility complex (MHC) class I, but not CD45 or MHC class II. (E, F, G) In vitro differentiation of rBM-MSCs. **(E)** The rBM-MSCs differentiated into the adipogenic lineage after 17 days of incubation. **(F)** Adipogenic differentiation was identified by neutral lipid vacuole formation (stained with Oil Red O), arrows) (green, actin) in cultures (scale bar, 50 μm). **(G)** Osteogenic differentiation of rBM-MSCs (day 8) after osteogenic induction. Mineral nodules were stained positive (arrows) with Alizarin Red S stain.

groups treated with MSC or VEGF + MSC (score 1 and 2). Severe fibrosis was observed in the peritubular interstitium of the UUO group (score 3), but light fibrosis was reduced in the groups treated with MSC or VEGF + MSC (score 1), and mild fibrosis was reduced in the VEGF-treated group (score 1) (Masson trichrome stain) (Table 1, Figures 2 and 3).

Transforming growth factor β-1, E-cadherin, nitric oxide, and hydroxyproline levels

We determined the effects of MSCs alone and MSCs transfected with VEGF on the levels of TGF-β1, E-cadherin, NO, and hydroxyproline in kidney tissue samples of rats with UUO. Levels of TGF-β1, E-cadherin ($P \leq .001$), and NO ($P \leq .05$) were significantly higher in group2 than studies groups (groups 2 and 3). Hydroxypyroline levels were higher in the UUO group 2, but there was no significant difference between the other groups (Table 2).

Figure 2. Representative Kidney Sections From Control and Experimental Groups

(A) Control kidney cortex showed absence of fibrosis in normal tissue. There was no histopathologic change in the glomeruli (g) and tubules (hematoxylin-eosin; original magnification ×100). **(B)** In the unilateral ureteral obstruction (UUO) group, there was severe total tubular necrosis, tubular degeneration, and epithelial vacuolization in the proximal tubules (score 4) and leukocyte infiltration (*) in the peritubular interstitium (score 3) (hematoxylin-eosin; original magnification ×100). **(C, D)** All the histopathologic alterations noted in the UUO group **(B)** were decreased in **(C)** the group with UUO and mesenchymal stem cells (MSC) (UUO + MSC) and **(D)** the group with UUO and vascular endothelial growth factor (VEGF) and MSC (UUO + VEGF + MSC). Leukocyte infiltration was reduced in the MSC-treated groups (*). Slight epithelial vacuolization was observed in the proximal tubules (black arrows) and normal glomeruli (hematoxylin-eosin; original magnification ×200).

Figure 3. Renal Histopathologic Scores of Experimental Groups
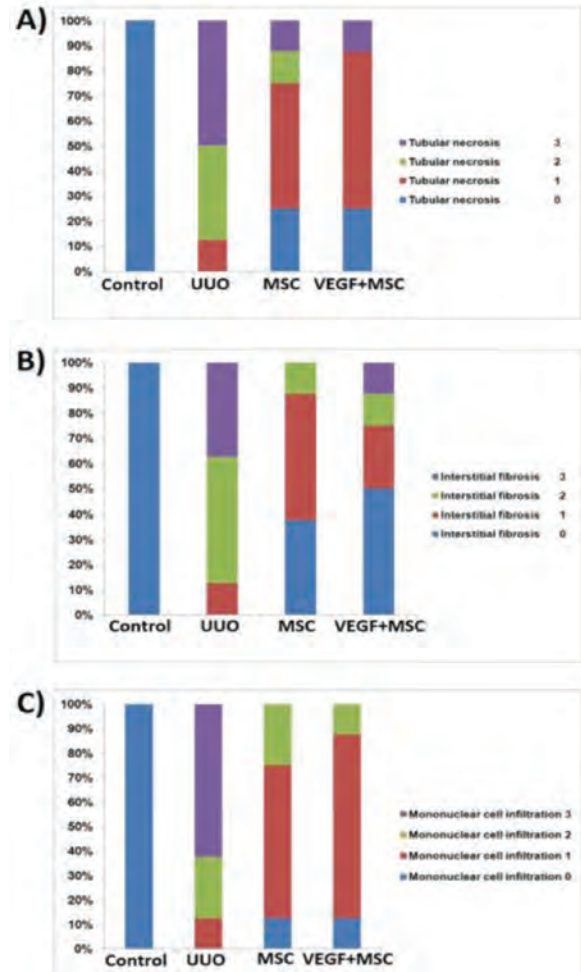
Abbreviations: MSC, mesenchymal stem cell; UUO, unilateral ureteral obstruction; VEGF, vascular endothelial growth factor
(A) Tubular necrosis. **(B)** Interstitial fibrosis. **(C)** Mononuclear cell infiltration. Scores: 0, no degeneration; 1, middle generation; 2, moderate degeneration; and 3, severe degeneration.

Table 1. Left Kidney Histopathologic Scores at Study Termination*						
Groups	Control (Group 1)	UUO (Group 2)	UUO + MSC (Group 3)	UUO + VEGF + MSC (Group 4)	$P \leq$ †	$P \leq$ ‡
Tubular necrosis	0	2.4 (1-3)	1.1 (0-3)	1 (0-3)	.001	.001
Interstitial fibrosis	0	2.3 (1-3)	0.8 (0-2)	0.9 (0-2)	.001	.001
Mononuclear cell infiltration	0	2.5 (1-3)				
	1.1 (0-2)					
	1 (0-2)	.001		.001		

Abbreviations: MSC, mesenchymal stem cell; UUO, unilateral ureteral obstruction; VEGF, vascular endothelial growth factor
*N = 8 rats/group. Scored from 0 to 3. Data reported as mean (range, minimum-maximum).
†Comparison between groups 2 and 3.
‡Comparison between groups 2 and 4.

Table 2. Assay Levels in Left Kidney Tissue*

Parameters	Control (Group 1)	UUO (Group 2)	UUO + MSC (Group 3)	UUO + VEGF + MSC (Group 4)
TGF-β1 (pg/mL)	2.5 ± 0.6	7.2 ± 1.5	3.8 ± 0.9[†]	4.1 ± 0.9[†]
E-cadherin (ng/mL)	3.7 ± 0.5	7.4 ± 1.2	4.1 ± 0.6[†]	4 ± 0.9[†]
NO (μmol/g)	20.6 ± 3.5	62.3 ± 19.8	26.6 ± 8.9[‡]	32 ± 8.8[‡]
Hydroxyproline (pg/mL)	357.5 ± 84.9	434.1 ± 51.8	423.5 ± 63.8	426.9 ± 62.1

Abbreviations: MSC, mesenchymal stem cell; NO, nitrous oxide; TGF-β1, transforming growth factor β1; UUO, unilateral ureteral obstruction; VEGF, vascular endothelial growth factor

*N = 8 rats/group. Data reported as mean ± SD.
[†]Significantly different from UUO group; $P \leq .001$.
[‡]Significantly different from UUO group; $P \leq .05$.

Detection of cells positive for green fluorescent protein and vascular endothelial growth factor in kidney tissue

Stem cells were administered intravenously (inferior vena cava) because of the unique accessibility of the kidney from the vascular network. After the left kidneys were excised, tissues were screened for the presence of GFP-positive and GFP-positive/VEGF-positive MSCs. In the tissue sections, MSCs expressing GFP and VEGF were spread through the kidney in the MSC-treated group, and the cells were discovered in the tubules, glomeruli, interstitial regions, and perivascular areas (Figures 4 and 5). In both groups with GFP-positive and GFP-positive/VEGF-positive rBM-MSCs, the expression levels of proinflammatory and anti-inflammatory cytokines were altered. To assess this change, sections were analyzed for the expression of anti-inflammatory (Prostaglandin E2 Receptor (EP3), IL-1RA), pro- and anti-inflammatory (IL-6), and

Figure 4. Effects of Mesenchymal Stem Cells (MSCs) Alone and Transfected With Vascular Endothelial Growth Factor (VEGF) on the Levels of Transforming Growth Factor β1 (TGF-β1), E-Cadherin, Nitric Oxide (NO), and hydroxypyrrolidine (OH-Pyrroline) in Kidney Tissue in Rats With Unilateral Ureteral Obstruction (UUO)
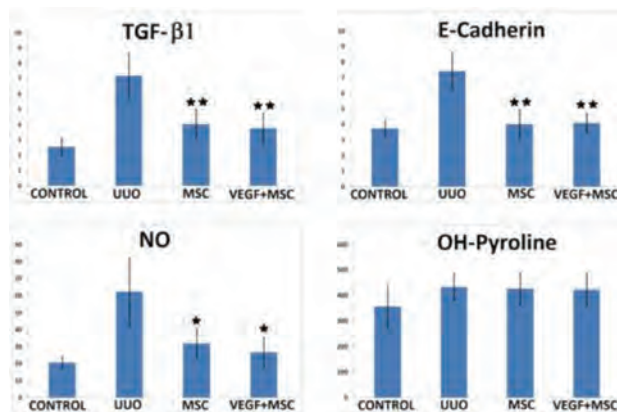
The TGF-β1, NO, and E-cadherin levels were significantly greater in the UUO than control the group; however, these values were significantly lower in the treated groups than in the UUO group. The OH-pyrroline levels were higher in the UUO group, but results were not significant compared with other groups (comparison with UUO group:*$P \leq .05$; **$P \leq .001$).

Figure 5. Mesenchymal Stem Cell (MSC) Infiltration and Vascular Endothelial Growth Factor (VEGF) Expression in Renal Tissue Sections After Venous Delivery
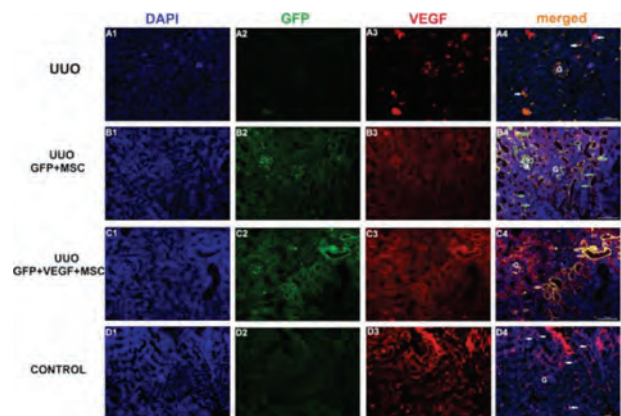
The MSCs labeled with green fluorescent protein (GFP) (green-stained cells; arrows) were localized to the renal tubules and interstitium of the kidney at 2 weeks after unilateral ureteral obstruction (UUO) (UUO + MSC) (B2 and B4) and VEGF + GFP + MSC group (C2 and C4). In control or phosphate-buffered saline-treated rats with UUO, all-green fluorescent staining represented background (A2 and D2); in the UUO + GFP + MSC and UUO + GFP + VEGF + MSC groups, the cytoplasmic micronuclear counterstains confirmed MSC migration to tubules and the interstitial compartment (orange or green cytoplasm/nuclei; arrows). The GFP-positive and VEGF-positive MSCs also were observed in the tubules (C4). The VEGF immunoreactivity was slightly positive in the UUO group, despite strongly positive staining in both groups including GFP + MSC and GFP + VEGF + MSC groups. The expression levels of VEGF were positive in the control group, especially in the tubules (DAPI, 4',6-diamidino-2-phenylindole).

proinflammatory (MPO) cytokines. The expression of EP3 and IL-1RA were significantly increased in the tissue of the groups injected with MSCs (with or without VEGF), but the same expression was observed weakly in the UUO group 2 (Figure 6). The cytokine IL-6 was strongly expressed in the tubules of rats that had UUO and treatment with MSCs with or without VEGF (Figure 6); this cytokine is the predominant mediator of the acute phase response triggered by inflammation, but it also functions as an anti-inflammatory factor. After the administration of MSCs with or without VEGF, cytokine expression levels (IL-1RA, EP3, and IL-6) in rats with UUO were significantly increased (Figure 6), and a reduction in MPO expression was observed (Figure 4). However,

Figure 6. Rat Kidney Tissue Sections Stained for Green Fluorescent Protein (GFP) and Vascular Endothelial Growth Factor (VEGF) in Different Groups
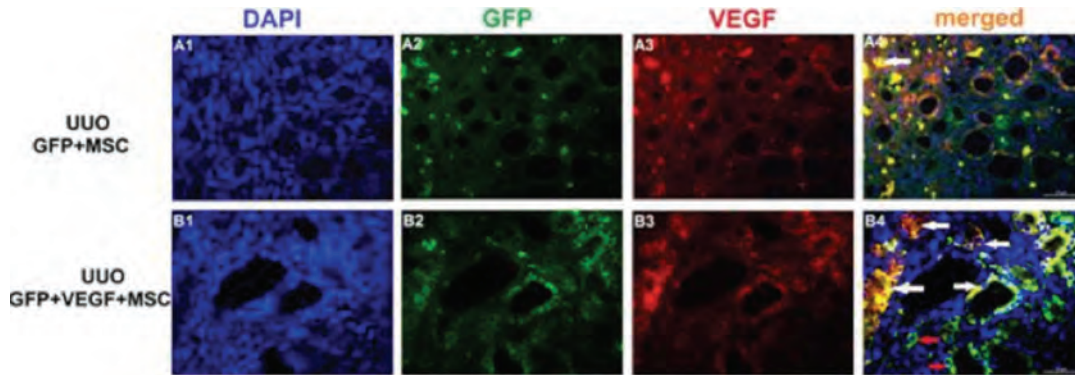

Abbreviations: DAPI, 4',6-diamidino-2-phenylindole; UUO, unilateral ureteral obstruction
(A1-A4) Rats treated with mesenchymal stem cells (MSCs).
(B1-B4) Rats treated with VEGF-transfected MSCs. Alteration in VEGF protein expression was observed in renal tissues of rats treated with VEGF-transfected MSCs (B4).

the expression of MPO was increased in the sections of the rats without cell injection (Figure 6). In tissue samples from rats transplanted with stem cells, the EP3, IL-1RA, and IL-6 levels were high, but MPO expression levels were low (Figure 7).

Figure 7. Expression of Anti-Inflammatory and Proinflammatory Cytokines in Kidney Paraffin Sections in Rats with Unilateral Ureteral Obstruction (UUO), Control Rats, and Rats Transplanted with Mesenchymal Stem Cells (MSCs)
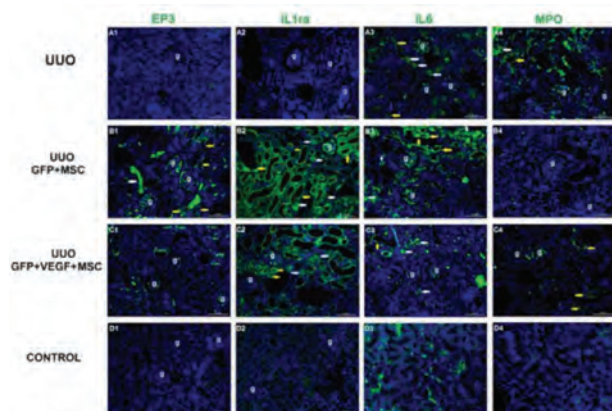
Abbreviations: GFP, green fluorescent protein; IL-1RA, interleukin 1 receptor antagonist; IL-6, interleukin 6; MPO, myeloperoxidase; MSC, mesenchymal stem cell; UUO, unilateral ureteral obstruction; VEGF, vascular endothelial growth factor)
Higher expression of EP3, IL-1RA and IL-6 was observed in the tissues of MSC groups compared with the UUO and control groups. In contrast, the expression of the proinflammatory cytokine MPO was reduced in MSC groups.

Discussion

Paracrine and autocrine effects are believed to be important for the therapeutic effects of MSCs beyond their differentiation into injured tissue cell types. The MSCs at injured tissue environments secrete several cytokines and growth factors that have paracrine and autocrine activities.[20,21] Nephrons and collecting ducts are of mesenchymal origin, and MSCs do not transdifferentiate into a malignant phenotype after transplant; therefore, the MSC therapy has great potential for renal repair.[22,23] The targeting of MSCs into the damaged tissue site by increased chemokine concentrations at the site of inflammation was well characterized, and intravenously injected MSCs migrate to the glomeruli, interstitium, peritubular capillaries, and tubules in both acute and chronic kidney injury models.[7,8,24,25]

There have been many studies that address transplanted systemic MSC therapy for healing kidney damage or injury. Yet, these studies have not investigated the effect of MSCs + VEGF treatment. The literature has limited studies about the effects of stem cell therapy on healing parameters. The present study showed that MSCs can be engrafted safely and successfully after injection into kidney tissue. The labelled MSCs were observed within the left kidney tissue. The staining results demonstrated that MSCs were well incorporated into obstructed kidneys, localizing primarily to the interstitial space and renal tubules, and were retained for up to 2 weeks after injection. Our results demonstrate that venous GFP-positive and GFP-positive/VEGF-positive MSCs were observed in the tubules, glomeruli, interstitial regions, and perivascular areas.

The expression of VEGF was significantly greater in the GFP-positive and GFP-positive/VEGF-positive MSC-transplanted groups than the UUO group. The VEGF is a potent angiogenic factor, and endogenous VEGF and its receptors are induced in ischemic tissues.[26-29] However, the function of VEGF in the

normal adult kidney and renal disease is unknown. The induction of vascular permeability, monocyte chemotaxis, and vasodilation by VEGF has been implicated in the pathogenesis of kidney disease,[30-32] but other studies have suggested that VEGF has a protective effect in thrombotic microangiopathy and crescentic glomerulonephritis.[33,34] An analysis of the effect of VEGF inhibition on renal structure and function under physiologic conditions showed that VEGF might protect the kidney from the injurious effects of hypertension and the renin-angiotensin system.[35]

In the presence of exogenous MSCs, VEGF gene expression was significantly reduced in response to obstruction. Similarly, we determined that the expression of VEGF protein was decreased in our UUO group than the control group. However, GFP-positive and GFP-positive/VEGF-positive MSCs could be incorporated into the tubules of the injured kidney. These results suggest that VEGF from MSCs or VEGF-positive MSCs (exogenously derived VEGF) might involve kidney repair after acute injury.

The second finding in our study was the immuno-modulation in the groups with GFP-positive and GFP-positive/VEGF-positive MSCs. We evaluated the expression of anti-inflammatory (IL-1RA, EP3), proinflammatory (MPO), and pro- and anti-inflammatory (IL-6) cytokines in kidney tissue samples of all groups. The expression levels of EP3 and IL-1RA were significantly increased in the tissue of the MSC-injected group, but the same expression in the control and UUO groups was weak. The EP3, a receptor for prostaglandin E2 (a major renal cyclooxygenase product of arachidonic acid metabolism), is expressed in renal vessels, the thick ascending limb, and the collecting duct. The EP3 has at least 6 alternative splice variants that couple to Gi proteins to inhibit cyclic adenosine monophosphate, inhibiting sodium and water transport.[36] The EP3 has both proinflammatory and anti-inflammatory effects in skin inflammation in rodents and humans, and EP3 signalling stimulation suppresses skin inflammation in murine contact hypersensitivity.[36]

The cytokine IL-1 is an important proinflammatory cytokine that has a wide range of effects, including the activation of endothelial cells, stimulation of tissue infiltration by neutrophils and macrophages, and induction of other mediators of inflammation such as tumor necrosis factor α and NO.[37] Its pathologic role has been identified in glomerulonephritis.[37,38]

Glomerular and tubular epithelial cells may be the origin of IL-1. Alternatively, IL-1RA may suppress IL-1 activity.[38,39] The site-specific delivery of the IL-1RA gene into inflamed glomeruli by bone marrow-derived cells as a vehicle suppresses local IL-1 action and prevents the progress of disease. Similarly, interstitial inflammation and fibrosis in obstructive nephro-pathy in tubulointerstitial injury was attenuated by the delivery of the IL-1RA gene by CD11b-positive vehicle cells. Anti-inflammatory mediators such as interleukin 10 (IL-10), IL-1RA, and interleukin 13 (IL-13) are increased after MSC treatment. The IL-1RA inhibits IL-1 and IL-1 attracts neutrophils, macrophages, and lymphocytes, resulting in tissue inflammation and the maintenance of epithelial cell survival.[40,41] Our results indicated that EP3 and IL-1RA expression levels were significantly increased in the kidney of the MSC-treated groups, which could cause beneficial effects in injured kidney tissue.

The oxide NO is an important mediator in UUO. In our previous experiment, we showed that UUO decreased NO production and that melatonin increased its production.[18] In previous experiments using MSCs in a UUO model, the role of NO was not studied. In the present study, we showed the positive effect of MSCs on NO production in UUO.

The EMT may be the major pathophysiologic mechanism responsible for UUO-induced renal injuries.[42] The EMT is the leading hypothesis for the origin of tubulointerstitial myofibroblasts.[43] Using biochemical assays, we measured renal cortical E-cadherin, TGF-β1, hydroxyproline, and NO levels as evidence of EMT. Levels of TGF-β1, E-cadherin, and NO levels were higher in the UUO group; however, in the study group, these values were significantly lower. Previous studies showed that E-cadherin levels were lower after UUO.[5-7] In our experiment, E-cadherin levels were higher after UUO and were reduced in the treated rats compared with the control group; however, the values in the treated group were higher than the control group. Similarly, hydroxyproline values were higher in the UUO group, but in treated rats, these values were lower, and no difference observed in all groups.

The MSCs spontaneously secrete TGF-β1, hepa-tocyte growth factor, and IL-6 but not interferon γ, IL-4, IL-5, or IL-10 in vitro.[44,45] Soluble factors secreted by MSCs that modulate inflammation and angiogenesis are significantly involved in tissue repair.[46] We previously reported that the cocultivation

of rBM-MSCs with islets and streptozotocin-damaged islets led to an increase in IL-6 and TGF-β1 into the culture supernatant compared with monocultures of rBM-MSCs, islets, and streptozotocin-damaged islets. The secretion of these cytokines by MSCs could have an effect in their anti-inflammatory or antiapoptotic function.[17]

In this study, the expression of IL-6 in kidney tissue was increased after MSC injection. These results suggest that the IL-6 in kidney parenchyma might be responsible for MSC-induced renal recovery after UUO-induced damage of the kidney. In a previous study, increased MPO activity and inflammation (infiltration of leukocytes and proinflammatory cytokines) caused oxidative stress and tissue damage in cisplatin-induced acute renal injury.[47] In our experiment, reduced kidney MPO activity after MSC injection indicated a possible decrease in neutrophil accumulation or activity. This finding indicates that MSCs could be a therapeutic approach as a potent immunosuppressive for the attenuation of histopathologic signs of UUO.

The present results showed that the anti-inflammatory and immunosuppressive effects of MSCs should be noted by a potential decrease of proinflammatory cytokines and an increase of anti-inflammatory cytokines. The treatment of UUO-induced renal EMT and renal fibrosis caused by exogenous MSCs and MSCs transfected with VEGF may affect kidney healing by the delivery of growth factors and cytokines that may improve some parameters. By understanding paracrine activity mediated by VEGF-positive MSCs and by elucidating the mechanisms of stem cell activation, it may be possible to develop effective clinical therapies to prevent UUO-induced renal damage. Currently, stem cells are used for the treatment of organ failure and regenerative therapy. Stem cells, especially allograft stem cells, may be used as an alternative therapy in the treatment of acute and chronic renal failure. Further clinical studies are needed to achieve a better understanding of the benefits and risks of MSC therapeutic use in clinical settings long term.

References

1. Klahr S, Morrissey J. Obstructive nephropathy and renal fibrosis. *Am J Physiol Renal Physiol*. 2002;283(5):F861-F875.
2. Eddy AA. Molecular insights into renal interstitial fibrosis. *J Am Soc Nephrol*. 1996;7(12):2495-2508.
3. Strutz F, Okada H, Lo CW, et al. Identification and characterization of a fibroblast marker: FSP1. *J Cell Biol*. 1995;130(2):393-405.
4. Zeisberg M, Strutz F, Müller GA. Renal fibrosis: an update. *Curr Opin Nephrol Hypertens*. 2001;10(3):315-320.
5. Dendooven A, Ishola DA Jr, Nguyen TQ, et al. Oxidative stress in obstructive nephropathy. *Int J Exp Pathol*. 2011;92(3):202-210.
6. Houghton DC, Plamp CE 3rd, DeFehr JM, Bennett WM, Porter G, Gilbert D. Gentamicin and tobramycin nephrotoxicity. A morphologic and functional comparison in the rat. *Am J Pathol*. 1978;93(1):137-152.
7. Herrera MB, Bussolati B, Bruno S, et al. Exogenous mesenchymal stem cells localize to the kidney by means of CD44 following acute tubular injury. *Kidney Int*. 2007;72(4):430-4041.
8. Ninichuk V, Gross O, Segerer S, et al. Multipotent mesenchymal stem cells reduce interstitial fibrosis but do not delay progression of chronic kidney disease in collagen4A3-deficient mice. *Kidney Int*. 2006;70(1):121-129.
9. Asanuma H, Vanderbrink BA, Campbell MT, et al. Arterially delivered mesenchymal stem cells prevent obstruction-induced renal fibrosis. *J Surg Res*. 2011;168(1):e51-e59.
10. Liu X, Shen W, Yang Y, Liu G. Therapeutic implications of mesenchymal stem cells transfected with hepatocyte growth factor transplanted in rat kidney with unilateral ureteral obstruction. *J Pediatr Surg*. 2011;46(3):537-545.
11. Bai ZM, Deng XD, Li JD, et al. Arterially transplanted mesenchymal stem cells in a mouse reversible unilateral ureteral obstruction model: in vivo bioluminescence imaging and effects on renal fibrosis. *Chin Med J* (Engl). 2013;126(10):1890-1894.
12. Liu YL, Wang YD, Zhuang F, et al. Immunosuppression effects of bone marrow mesenchymal stem cells on renal interstitial injury in rats with unilateral ureteral obstruction. *Cell Immunol*. 2012;276 (1-2):144-152.
13. Ohnishi S, Sumiyoshi H, Kitamura S, Nagaya N. Mesenchymal stem cells attenuate cardiac fibroblast proliferation and collagen synthesis through paracrine actions. *FEBS Lett*. 2007;581(21):3961-3966.
14. Ortiz LA, Gambelli F, McBride C, et al. Mesenchymal stem cell engraftment in lung is enhanced in response to bleomycin exposure and ameliorates its fibrotic effects. *Proc Natl Acad Sci U S A*. 2003; 100(14):8407-8411.
15. Rojas M, Xu J, Woods CR, et al. Bone marrow-derived mesenchymal stem cells in repair of the injured lung. *Am J Respir Cell Mol Biol*. 2005;33(2):145-152.
16. Yilmaz S, Inandiklioglu N, Yildizdas D, et al. Mesenchymal stem cell: does it work in an experimental model with acute respiratory distress syndrome? *Stem Cell Rev*. 2013;9(1):80-92.
17. Karaoz E, Genç ZS, Demircan PÇ, Aksoy A, Duruksu G. Protection of rat pancreatic islet function and viability by coculture with rat bone marrow-derived mesenchymal stem cells. *Cell Death Dis*. 2010;1:e36.
18. Ozbek E, Ilbey YO, Ozbek M, Simsek A, Cekmen M, Somay A. Melatonin attenuates unilateral ureteral obstruction-induced renal injury by reducing oxidative stress, iNOS, MAPK, and NF-kB expression. *J Endourol*. 2009;23(7):1165-1173.
19. Menaka KB, Ramesh A, Thomas B, Kumari NS. Estimation of nitric oxide as an inflammatory marker in periodontitis. *J Indian Soc Periodontol*. 2009;13(2):75-78.
20. Xu YX, Chen L, Wang R, et al. Mesenchymal stem cell therapy for diabetes through paracrine mechanisms. *Med Hypotheses*. 2008; 71(3):390-393.
21. Ichim TE, Alexandrescu DT, Solano F, et al. Mesenchymal stem cells as anti-inflammatories: implications for treatment of Duchenne muscular dystrophy. *Cell Immunol*. 2010;260(2):75-82.
22. Le Blanc K. Immunomodulatory effects of fetal and adult mesenchymal stem cells. *Cytotherapy*. 2003;5(6):485-489.
23. Jiang Y, Jahagirdar BN, Reinhardt RL, et al. Pluripotency of mesenchymal stem cells derived from adult marrow. *Nature*. 2002; 418(6893):41-49. Erratum in: *Nature*. 2007;447(7146):879-880.
24. Devine SM, Bartholomew AM, Mahmud N, et al. Mesenchymal stem cells are capable of homing to the bone marrow of non-human primates following systemic infusion. *Exp Hematol*. 2001;29(2):244-255.

25. Wong CY, Cheong SK, Mok PL, Leong CF. Differentiation of human mesenchymal stem cells into mesangial cells in post-glomerular injury murine model. *Pathology.* 2008;40(1):52-57.

26. Carmeliet P. Basic Concepts of (Myocardial) Angiogenesis: Role of Vascular Endothelial Growth Factor and Angiopoietin. *Curr Interv Cardiol Rep.* 1999;1(4):322-335.

27. Takeshita S, Zheng LP, Brogi E, et al. Therapeutic angiogenesis. single intraarterial bolus of vascular endothelial growth factor augments revascularization in a rabbit ischemic hind limb model. *J Clin Invest.* 1994;93(2):662-670.

28. Zhang ZG, Zhang L, Jiang Q, et al. VEGF enhances angiogenesis and promotes blood-brain barrier leakage in the ischemic brain. *J Clin Invest.* 2000;106(7):829-838.

29. Vincent KA, Shyu KG, Luo Y, et al. Angiogenesis is induced in a rabbit model of hind limb ischemia by naked DNA encoding an HIF-1alpha/VP16 hybrid transcription factor. *Circulation.* 2000;102 (18):2255-2261.

30. Senger DR, Galli SJ, Dvorak AM, Perruzzi CA, Harvey VS, Dvorak HF. Tumor cells secrete a vascular permeability factor that promotes accumulation of ascites fluid. *Science.* 1983;219 (4587):983-985.

31. Barleon B, Sozzani S, Zhou D, Weich HA, Mantovani A, Marmé D. Migration of human monocytes in response to vascular endothelial growth factor (VEGF) is mediated via the VEGF receptor flt-1. *Blood.* 1996;87(8):3336-3343.

32. Ku DD, Zaleski JK, Liu S, Brock TA. Vascular endothelial growth factor induces EDRF-dependent relaxation in coronary arteries. *Am J Physiol.* 1993;265(2 Pt 2):H586-H592.

33. Kim YG, Suga SI, Kang DH, et al. Vascular endothelial growth factor accelerates renal recovery in experimental thrombotic microangiopathy. *Kidney Int.* 2000;58(6):2390-2399.

34. Hara A, Wada T, Furuichi K, et al. Blockade of VEGF accelerates proteinuria, via decrease in nephrin expression in rat crescentic glomerulonephritis. *Kidney Int.* 2006;69(11):1986-1995. Erratum in: *Kidney Int.* 2006;70(9):1666.

35. Advani A, Kelly DJ, Advani SL, et al. Role of VEGF in maintaining renal structure and function under normotensive and hypertensive conditions. *Proc Natl Acad Sci U S A.* 2007;104(36):14448-14453.

36. Honda T, Matsuoka T, Ueta M, Kabashima K, Miyachi Y, Narumiya S. Prostaglandin E(2)-EP(3) signaling suppresses skin inflammation in murine contact hypersensitivity. *J Allergy Clin Immunol.* 2009;124 (4):809-818.e2.

37. Goulet JL, Pace AJ, Key ML, et al. E-prostanoid-3 receptors mediate the proinflammatory actions of prostaglandin E2 in acute cutaneous inflammation. *J Immunol.* 2004;173(2):1321-1326.

38. Atkins RC, Nikolic Paterson DJ, Lan HY. Tubulointerstitial injury in glomerulonephritis. *Nephrology.* 1996;2(suppl 1):S2-S6.

39. Boswell JM, Yui MA, Burt DW, Kelley VE. Increased tumor necrosis factor and IL-1 beta gene expression in the kidneys of mice with lupus nephritis. *J Immunol.* 1988;141(9):3050-3054.

40. Noronha IL, Krüger C, Andrassy K, Ritz E, Waldherr R. In situ production of TNF-alpha, IL-1 beta and IL-2R in ANCA-positive glomerulonephritis. *Kidney Int.* 1993;43(3):682-692.

41. Németh K, Leelahavanichkul A, Yuen PS, et al. Bone marrow stromal cells attenuate sepsis via prostaglandin E(2)-dependent reprogramming of host macrophages to increase their interleukin-10 production. *Nat Med.* 2009;15(1):42-49. Erratum in: *Nat Med.* 2009;15(4):462.

42. Volarevic V, Al-Qahtani A, Arsenijevic N, Pajovic S, Lukic ML. Interleukin-1 receptor antagonist (IL-1Ra) and IL-1Ra producing mesenchymal stem cells as modulators of diabetogenesis. *Autoimmunity.* 2010;43(4):255-263.

43. Higgins DF, Lappin DW, Kieran NE, et al. DNA oligonucleotide microarray technology identifies fisp-12 among other potential fibrogenic genes following murine unilateral ureteral obstruction (UUO): modulation during epithelial-mesenchymal transition. *Kidney Int.* 2003;64(6):2079-2091.

44. Park JH, Hwang I, Hwang SH, Han H, Ha H. Human umbilical cord blood-derived mesenchymal stem cells prevent diabetic renal injury through paracrine action. *Diabetes Res Clin Pract.* 2012;98(3):465-473.

45. Aksu AE, Horibe E, Sacks J, et al. Co-infusion of donor bone marrow with host mesenchymal stem cells treats GVHD and promotes vascularized skin allograft survival in rats. *Clin Immunol.* 2008;127(3):348-358.

46. Phinney DG, Prockop DJ. Concise review: mesenchymal stem/multipotent stromal cells: the state of transdifferentiation and modes of tissue repair--current views. *Stem Cells.* 2007;25(11): 2896-2902.

47. Mitazaki S, Honma S, Suto M, et al. Interleukin-6 plays a protective role in development of cisplatin-induced acute renal failure through upregulation of anti-oxidative stress factors. *Life Sci.* 2011;88(25-26):1142-1148.